Local Expression of Indoleamine 2,3 Dioxygenase in Syngeneic Fibroblasts Significantly Prolongs Survival of an Engineered Three-Dimensional Islet Allograft

Reza B. Jalili,[1,2] Farshad Forouzandeh,[1] Alireza Moeen Rezakhanlou,[1] Ryan Hartwell,[1] Abelardo Medina,[1] Garth L. Warnock,[1] Bagher Larijani,[2] and Aziz Ghahary[1]

OBJECTIVE—The requirement of systemic immunosuppression after islet transplantation is of significant concern and a major drawback to clinical islet transplantation. Here, we introduce a novel composite three-dimensional islet graft equipped with a local immunosuppressive system that prevents islet allograft rejection without systemic antirejection agents. In this composite graft, expression of indoleamine 2,3 dioxygenase (IDO), a tryptophan-degrading enzyme, in syngeneic fibroblasts provides a low-tryptophan microenvironment within which T-cells cannot proliferate and infiltrate islets.

RESEARCH DESIGN AND METHODS—Composite three-dimensional islet grafts were engineered by embedding allogeneic mouse islets and adenoviral-transduced IDO–expressing syngeneic fibroblasts within collagen gel matrix. These grafts were then transplanted into renal subcapsular space of streptozotocin diabetic immunocompetent mice. The viability, function, and criteria for graft take were then determined in the graft recipient mice.

RESULTS—IDO-expressing grafts survived significantly longer than controls (41.2 ± 1.64 vs. 12.9 ± 0.73 days; $P < 0.001$) without administration of systemic immunesuppressive agents. Local expression of IDO suppressed effector T-cells at the graft site, induced a Th2 immune response shift, generated an anti-inflammatory cytokine profile, delayed alloantibody production, and increased number of regulatory T-cells in draining lymph nodes, which resulted in antigen-specific impairment of T-cell priming.

CONCLUSIONS—Local IDO expression prevents cellular and humoral alloimmune responses against islets and significantly prolongs islet allograft survival without systemic antirejection treatments. This promising finding proves the potent local immunosuppressive activity of IDO in islet allografts and sets the stage for development of a long-lasting nonrejectable islet allograft using stable IDO induction in bystander fibroblasts. ***Diabetes*** **59:2219–2227, 2010**

Endocrine replacement therapy by islet transplantation represents a feasible and attractive alternative therapeutic approach for treating type 1 diabetes (1,2). Despite improvement of allogeneic islet engraftment using systemic immunosuppression, islet transplantation is still limited by high rates of rejection. Furthermore, some immunosuppressive agents are prodiabetogenic and associated with adverse side effects (3–6). Finding more efficient and less harmful strategies to protect islet graft is therefore required for improving islet transplantation outcome.

Localized expression of immunoregulatory factors using gene transfer to graft is a feasible method to provide an immunoprivileged microenvironment and consequently improves graft survival. Such an on-site delivery system results in more potent local immunosuppression with less systemic side effects (7–9).

IDO is a cytosolic enzyme that catalyzes essential amino acid L-tryptophan to kynurenine (10) and has profound effects on T-cell proliferation, differentiation, effector functions, and viability (11). Both the reduction in local tryptophan concentration and the production of immunomodulatory tryptophan metabolites contribute to immunosuppressive effects of IDO (12,13). Broad evidence implicates IDO and the tryptophan catabolic pathway in generation of immune tolerance to antigens in tissue microenvironments. In particular, the role of IDO in fetal tolerance in mammalian pregnancy (14,15), immunologic tolerance to tumors (16,17), and self-tolerance has been documented (18,19). The unique immunoregulatory function of IDO substantiates the application of this enzyme as a strategy to suppress alloimmune responses in transplantation.

Our research group has shown that overexpression of IDO in fibroblasts suppresses immune response and improves outcome of skin grafts (20–25) and that bystander IDO-expressing fibroblasts suppress immune response to allogeneic mouse islets in vitro (26). Furthermore, in a recent study we showed that mouse islets and fibroblasts are selectively resistant to IDO-mediated activation of nutrient deficiency stress (27). Here, we engineered a three-dimensional composite islet allograft equipped with IDO-expressing fibroblasts and examined whether local expression of IDO, conferred by adenoviral-mediated gene transfer to bystander syngeniec fibroblasts, prevents the rejection of islet allograft. Our approach here is novel compared with other studies that examined the suppressive effect of IDO in islet transplantation (28,29) because *1*) bystander syngeneic fibroblasts were used as the target of gene transfer instead of islets to avoid deleterious effects of adenovirus infection on islets (30–32), *2*) islets were embedded within an extracellular matrix that by itself improves islet function and viability (33,34), and *3*) cotransplanted fibroblasts are more than just a source of IDO and can enhance islet physiological competence (35,36).

From the [1]Department of Surgery, University of British Columbia, Vancouver, British Columbia, Canada; and the [2]Endocrinology and Metabolism Research Center, Medical Sciences, University of Tehran, Tehran, Iran.
Corresponding author: Aziz Ghahary, aghahary@interchange.ubc.ca.
Received 22 October 2009 and accepted 19 May 2010. Published ahead of print at http://diabetes.diabetesjournals.org on 3 June 2010. DOI: 10.2337/db09-1560.

See accompanying commentary, p. 2102.

TABLE 1
Composite islet graft survival in different experimental groups

	n	Graft survival (days posttransplantation)	Mean ± SE	*P**
Islet plus untreated fibroblasts	10	10, 11, 12 (×2), 13, 14, 15 (×2), 16, and 17	13.5 ± 0.79	0.706
Islet plus mock vector fibroblasts	10	10, 11, 12 (×2), 13, 14 (×2), 15 (×2), and 16	13.2 ± 0.61	0.908
Islet plus IDO fibroblasts	10	33, 36, 38 (×2), 41, 42, 43, 45 (×2), and 51	41.2 ± 1.64	<0.001
Islet alone	10	10, 11 (×2), 12 (×3), 13, 15, 16, and 17	12.9 ± 0.73	—

*Difference in mean survival durations compared with the islet-alone group, calculated using log-rank (Mantel-Cox) test.

RESEARCH DESIGN AND METHODS

Mouse islet isolation and preparation of three-dimensional islet-fibroblast composite grafts. Islets were isolated from 6- to 8-week-old male BALB/c mice (The Jackson Laboratories, Bar Harbor, ME), and mouse dermal fibroblasts were explanted from B6 mice skin and transduced with a recombinant adenoviral vector carrying human IDO cDNA as previously described (26). Control fibroblasts were infected with a mock vector or left untreated. Fibroblast-populated collagen gel (FPCG) matrices were prepared as described by Sarkhosh et al. (23) using IDO-expressing or control fibroblasts. Mouse islets were added to FPCG before solidification in 24-well plates. Care and maintenance of all animals were in accordance with the principals of laboratory animal care and the guidelines of the institutional Animal Policy and Welfare Committee.

Transplantation of islet-fibroblast composite grafts and evaluation of graft function. Recipient C57BL/6 (B6) mice were rendered diabetic by a single intraperitoneal injection of 200 mg/kg streptozotocin (Sigma), and diabetes was defined as a minimum of two consecutive blood glucose measurements ≥20 mmol/l. Islet plus IDO-expressing or control fibroblast composite grafts (~500 islets) were transplanted under the left kidney capsule of isoflurane-anesthetized diabetic mice. After transplantation, blood glucose levels were measured using an Accu-Chek Compact Plus blood glucose monitoring system, and grafts were deemed functioning when blood glucose levels decreased to <10 mmol/l. Intraperitoneal glucose tolerance tests (IPGTT) were performed as previously described (27) 2 and 4 weeks after transplantation. All animals were cared for according to the guidelines of the institutional Animal Policy and Welfare Committee.

Histological analyses and immunostainings. Graft-bearing kidneys or draining lymph nodes were harvested at indicated time points, fixed in 10% buffered formalin solution, and embedded in paraffin. Sections 5-μm thick from graft area were stained with hematoxylin-eosin (H-E). Immunofluorescence staining was performed for insulin, CD3, FOXP3, and IDO. Sections were rehydrated, and nonspecific binding was blocked. Sections were incubated overnight at 4°C with appropriate primary antibodies and then washed and incubated with relevant secondary antibodies for 45 min. Primary antibodies include guinea pig anti-insulin antibody (1:500 dilution; Dako Laboratories, Mississauga, Ontario, Canada), rabbit anti-CD3 antibody (1:100 dilution; abcam, Cambridge, MA), rat anti-mouse FOXP3 (1:200 dilution; eBioscience, San Diego, CA), and rabbit anti-IDO antibody (1:1,000 dilution, raised in rabbit; Washington Biotechnology, Baltimore, MD). Secondary antibodies (1:2000 dilution) used were fluoroisothiocyanate (FITC) goat anti-guinea pig IgG (abcam), rhodamine goat anti-rabbit IgG (Chemicon International, Temecula, CA), and rhodamine goat anti-rat IgG (Jackson ImmunoResearch, West Grove, PA).

Characterization of graft-infiltrating cells. Composite grafts were harvested at indicated time points, and collagen matrices were digested using type I collagenase (1 mg/ml; Sigma) at 37°C for 10 min. Cell suspensions were washed with PBS and passed through a 40-μm cell strainer. Cells were then incubated for 30 min at 4°C with fluorescent-conjugated antibodies (1:100 dilutions; eBioscience) specific for particular lymphocyte and antigen-presenting cell (APC) markers. Fluorescence dot plots were created using a BD FACS Calibur flow cytometry machine (BD Biosciences Pharmingen, Mississauga, Ontario, Canada) and were used to determine the percentage of positive cells labeled with the corresponding antibodies.

Quantitative PCR. Total RNA was isolated from harvested grafts at indicated time points using an RNeasy kit (Qiagen). cDNA was synthesized using the SuperScript first-strand synthesis system for RT-PCR (Invitrogen, Carlsbad, CA) according to the manufacturer's protocol. Quantitative RT-PCR was performed in a reaction mixture of 25 μl using the Platinum SYBR Green qPCR SuperMix-UDG with ROX (Invitrogen) PCR kit according to the manufacturer's instructions. The reactions were run on a 7900 HT Fast Real time PCR system (Applied biosystems, Foster City, CA). Human IDO-specific and mouse cytokine and chemokine mRNAs were quantified relative to mouse glyceraldehyde-3-phosphate dehydrogenase (GAPDH) using primers listed in supplementary Table 1 (available in an online appendix [http://diabetes.diabetesjournals.org/cgi/content/full/db09-1560/DC1]). The analyses were performed with the Sequence Detection system 7900HT software (version 2.3; Applied biosystems). All measurements were performed in duplicate. Results are expressed as the percentage or fold increase in expression of mRNA of interest at the indicated time point compared with day one posttransplantation.

Serum alloantibody detection. Blood serum samples were collected from composite graft recipients B6 mice (H-2b) at indicated time points posttransplantation. Donor BALB/c mice (H-2d) thymocytes (1×10^6) were incubated with recipient B6 mouse serum at 1:128 dilution for 1 h at 37°C. Thymocytes were then washed with PBS and incubated with FITC-conjugated goat anti-mouse IgG1 or IgG2c (1:200 dilution; AbD Serotec, Raleigh, NC) for 1 h at 4°C. Binding of cells to antibody was detected from single-parameter fluorescence histograms using a BD FACSCanto flow cytometer (BD Biosciences) after gating on viable cells. Percentage of cells shifting into an appositive region on fluorescence histogram was calculated.

Mixed lymphocyte reaction. Stimulator cells were splenocytes from islet donor (BALB/c; H-2d) or third-party (C3H; H-2K) mouse strains, and responder cells were lymphocytes from graft-draining (renal) lymph nodes of graft-recipient mice (B6; H-2b). Responder cells (2×10^5) were cultured with irradiated (2000 rad) stimulator cells in 96-well round-bottom microtiter plates (Costar, Corning, NY) for 96 h. Individual wells were pulsed with 1 μCi/well of [^{3}H]-thymidine for the last 18 h. Culture plates were then harvested, and [^{3}H]-thymidine incorporation was measured using a Wallac Jet 1450 Microbeta scintillation counter (Perkin Elmer, Waltham, MA). Mean counts per minute were determined from cultures set up in triplicate.

Statistical analysis. Data are means ± SEM of three or more independent set of experiments. Survival of islet grafts in IDO-expressing versus control groups was compared using the Kaplan-Meier log-rank test. The statistical differences of mean values among treated and control groups were tested with one-way ANOVA. Post hoc comparisons were done using Student's *t* test with Bonferroni correction for multiple comparisons. *P* values <0.05 were considered statistically significant.

RESULTS

Local expression of IDO prolongs islet allograft survival and function. To investigate the local immunosuppressive effect of IDO, three-dimensional grafts were engineered by embedding 500 BALB/c mouse islets within collagen matrix populated with adenoviral-transduced IDO-expressing or control (mock vector infected or untreated) B6 mouse fibroblasts. IDO overexpression was validated in composite grafts (supplementary Fig. 1). These composite grafts where then transplanted to renal subcapsular space of streptozotocin-induced diabetic immune-competent B6 mice. Another control group of mice received only islets. Islet graft function was checked by measuring blood glucose in graft-recipient mice. Composite IDO-expressing grafts showed a significant prolongation of graft survival (41.2 ± 1.64 days; $P < 0.001$; $n = 10$ (Table 1 and Fig. *1A*). In contrast, as shown in Table 1 and Fig. 1*A*, control grafts were rejected within 2 weeks after transplantation. Mean duration of graft survival in islet-alone group and grafts with untreated and mock virus–treated fibroblast were 12.9 ± 0.73, 13.5 ± 0.79, and 13.2 ± 0.61 days, respectively (Table 1). Mean survival duration for mock vector–infected composite grafts was not significantly different from those of grafts with untreated fibro-

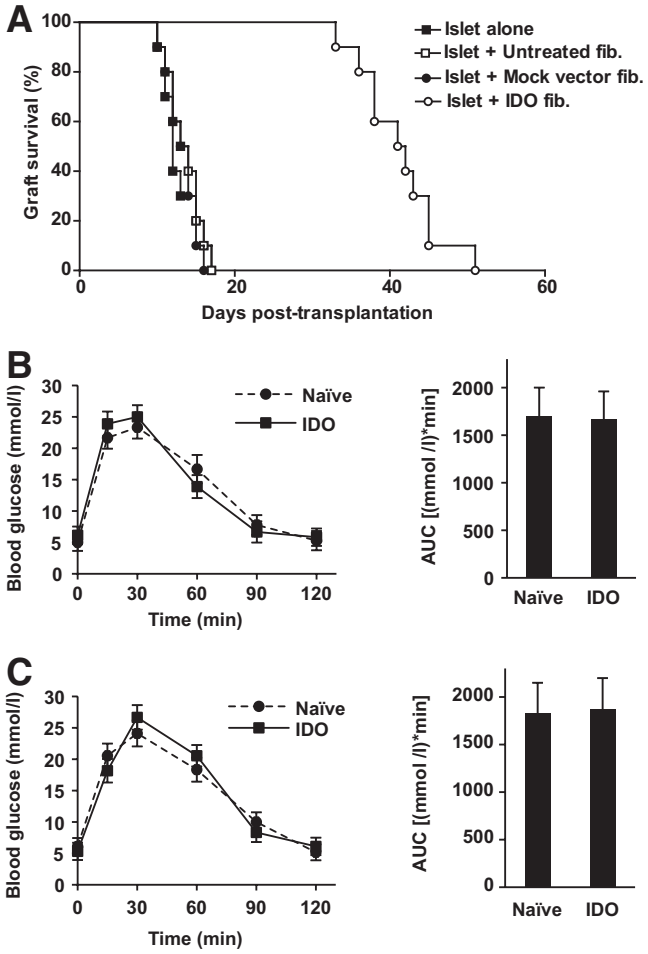

FIG. 1. Islet graft survival and function after transplantation. *A*: Kaplan-Meier survival curve shows prolongation of IDO-expressing grafts survival (solid line) compared with islet alone (dash-dot line), untreated (dashed line), and mock virus–infected (dotted line) grafts (n = 10). IPGTT after 2 weeks (*B*) and 4 weeks (*C*) posttransplantation confirmed normal glucose responsiveness in graft-bearing mice (solid line) vs. naïve mice (dashed line) (n = 3). Bar charts on the right panels show area under the IPGTT curves. Error bars indicate SEM.

blasts and islet-alone grafts, which confirmed that adenoviral infection by itself had no effect on graft survival.

IPGTT was performed on mice that received IDO-expressing composite grafts after 2 and 4 weeks posttransplantation. As shown in Fig. 1*B* and *C*, glucose clearance rates in mice received IDO-expressing grafts were comparable with age-matched naïve animals after 2 weeks (area under the curve 1,671.0 ± 289.1 vs. 1,700.1 ± 300.3 mmol · l^{-1} · min, respectively; $P > 0.05$) and 4 weeks (1,870.7 ± 327.8 vs. 1,824.2 ± 325.4 mmol · l^{-1} · min; $P > 0.05$) posttransplantation. Normal response of islet grafts to IPGTT demonstrated that islets in IDO-expressing composite grafts are able to function normally in response to glucose load, suggesting preservation of islet mass. These data collectively confirm that local IDO expression significantly prolongs islet allograft survival.

IDO prevents infiltration of lymphocytes into composite grafts. A set of graft recipient mice were killed at the end of each week posttransplantation to examine histopathological changes in islet allografts. Composite grafts were then recovered and stained with H-E or subjected to immunofluorescence staining for insulin, CD3, or FOXP3. Histological studies demonstrated that islets architecture was well preserved in the IDO-expressing composite grafts for up to 6 weeks (Fig. 2*G–L*), whereas islets in the untreated (Fig. 2*A–C*) or mock vector–infected grafts (Fig. 2*D–F*) were almost completely destroyed before the third week posttransplantation. Control grafts were diffusely infiltrated with mononuclear cells as early as the second week posttransplantation (Fig. 2*B* and *E*), while IDO-expressing grafts remained intact for up to 6 weeks (Fig. 2*G–K*). To investigate whether a component of immune response generated against adenovirus-infected syngeneic fibroblasts and/or human transgenic IDO, islet-free IDO-expressing or mock vector fibroblast–populated collagen matrices were transplanted to B6 mice. T-cell infiltration was not detected in IDO-expressing grafts after 40 days posttransplant, whereas IDO transgene was still expressed (supplementary Fig. 2).

Double staining of grafts for CD3 and insulin showed very few insulin-producing cells and dense T-cell infiltration in both untreated and mock vector–infected controls at the end of the second week posttransplantation (Fig. 3*A*). In contrast, islets in IDO-expressing grafts were strongly stained for insulin and maintained their normal architecture with minimal infiltration of T-cells at the same time point (two weeks posttransplant; Fig. 3*A*). A remarkable finding was that T-cells densely accumulated at the interface between IDO-expressing graft and kidney tissue but did not penetrate into the composite graft (IDO 2 weeks posttransplant [Figs. 2*I* and 3*A*]). However, T-cells started to infiltrate IDO vector–infected grafts by the end of the fifth week posttransplant (Fig. *3A*). While FOXP3 immunostaining revealed very few intragraft $FOXP3^+$ cells in all experimental groups (Fig. 3*B*), more $FOXP3^+$ cells were present in graft-draining lymph nodes of IDO-expressing recipients at week two but not week five posttransplant (Fig. 3*C*).

Flow cytometry was used to determine the specific T-cell and APC composition of the leukocyte infiltrates to the grafts. As shown in Fig. 4*A*, $CD4^+$ and $CD8^+$ T-cells were much more abundant in untreated (25.4 and 12.3%, respectively) and mock vector grafts (24.7 and 10.4%) compared with IDO-expressing grafts (3.3 and 3.4%) at 2 weeks posttransplant. Nonetheless, IDO grafts were accumulated with $CD4^+$ and $CD8^+$ T-cells by week five posttransplant (24.1 and 11.2%, respectively). Figure 4*B* summarizes flow cytometry data on graft-infiltrating cells composition. Because IDO has been shown to regulate APC function, the frequency of dendritic cells present in grafts was investigated. Results showed that although the frequency of $CD11c^+$ cells was less in IDO overexpressing grafts after 2 weeks (Fig. 4*A* and *B*), the ratio of $CD11c^+$ to $CD3^+$ cells was significantly higher in this group (Fig. 4*C*), suggesting that dendritic cells are more resistant than T-cells to IDO effects.

Taken together, these data show that local expression of IDO significantly prevents infiltration of T-cells into islet allografts and suggest local depletion of effctor $CD4^+$ and $CD8^+$ T-cells as a mechanism for an antirejection function of IDO.

Local IDO expression enhances anti-inflamatory Th2 type immune response and delays alloantibody production. To further investigate the mechanism of immunosuppression induced by IDO, we examined the local cytokine/chemokine expression profile and production of donor-specific alloantibodies in composite graft recipients. Quantitative PCR showed significantly higher proinflammatory cytokines γ-interferon, interleukin (IL)-2, and

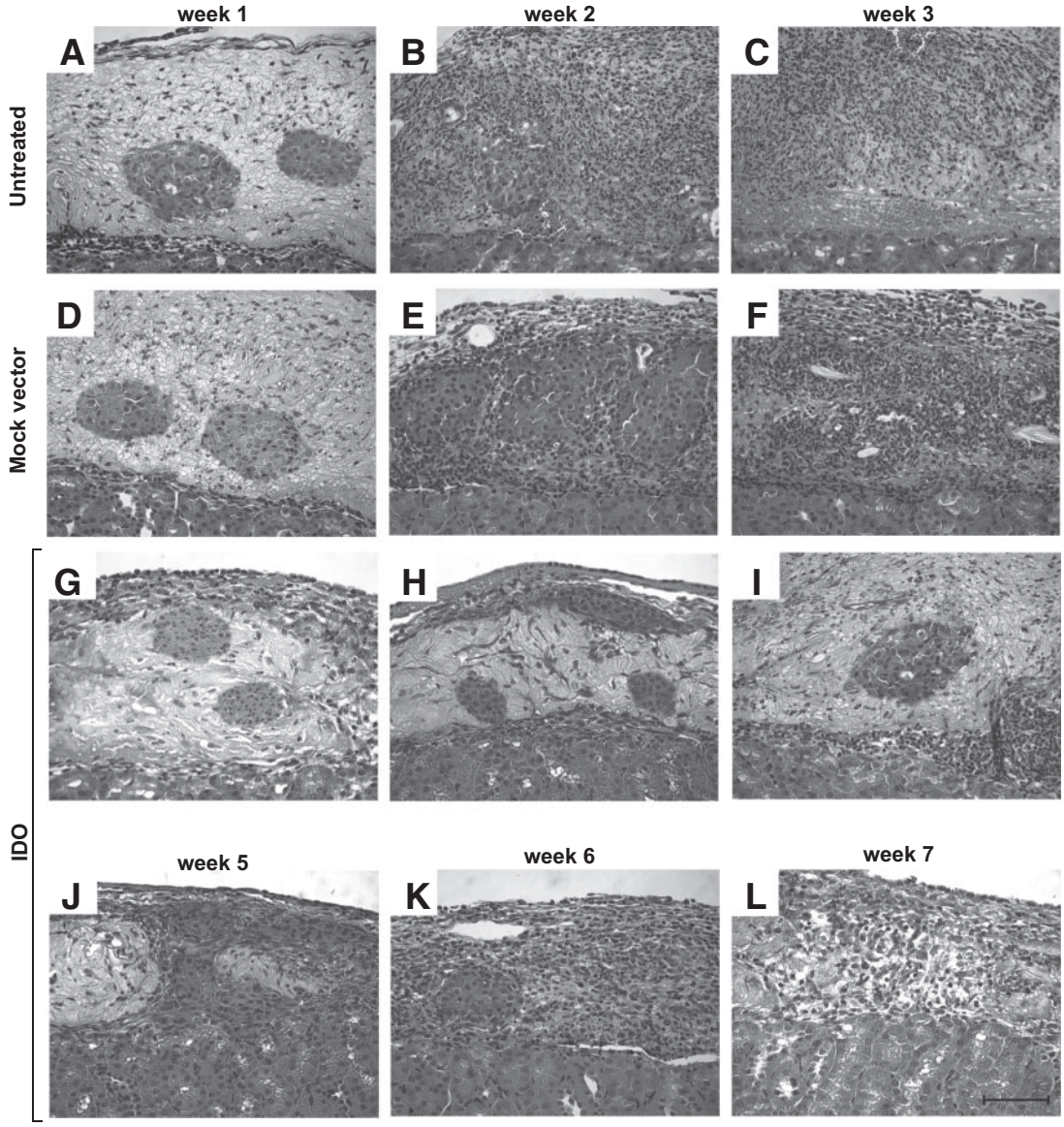

FIG. 2. Histology of composite islet grafts. Graft-recipient mice were killed at indicated time points posttransplantation. Composite islet grafts were then retrieved and stained with H-E. Untreated (*A–C*) and mock vector infected (*D–F*) fibroblast grafts after 1, 2, and 3 weeks posttransplantation, respectively. *G–L*: IDO-expressing fibroblast grafts after 1–3 and 5–7 weeks posttransplantation. Note that inflammation and cellular infiltration into the graft started in control groups in the second week but, in the IDO group, delayed until the sixth week posttransplantation. Scale bar: 100 μm.

IL-17 as well as T-cell–attracting chemokines CXCL9 and CXCL10 in untreated and mock vector grafts versus IDO-expressing grafts two weeks posttransplantation (Fig. 5*A*). Conversely, anti-inflammatory cytokines IL-4 and IL-10 were significantly overexpressed in IDO grafts at the same time point. However, cytokine/chemokine profile switched to a proinflammatory pattern after 5 weeks in the IDO group (Fig. 5*A*). Thus, low expression of T-cell–attracting chemokines and high levels of anti-inflammatory cytokines can be considered one of the reasons for strict containment of leukocyte infiltration into IDO-expressing grafts.

To investigate alloantibody production, flow cytometry was used to test sera from graft recipient animals for presence of antibodies against donor antigens. In control groups (i.e., mice receiving untreated or mock vector composite grafts), high levels of alloantibodies were detectable three weeks after transplantation (Fig. 5*B* and *C*). Higher levels of IGg2c versus IgG1 isotype was indicative of a Th1 dominant humoral immune response in these groups. In contrast, sera from IDO-expressing graft recipients showed low levels of donor-specific antibodies until the fifth week posttransplant, and it took two more weeks to reach to a level equal to that of the control groups at week three posttransplant (Fig. 5*D*). Moreover, early alloantibodies in IDO group were mainly from IgG1 subclass, suggesting a Th2 immune response shift in the presence of local IDO expression. These findings show that local IDO expression promotes an anti-inflammatory environment and shifts the Thl/Th2 balance toward Th2 response.

Allospecific T-cell priming is impaired in draining lymph nodes of IDO graft recipient mice. As shown in Fig. 3*C*, $FOXP3^+$ cells in graft-draining lymph nodes of IDO-expressing animals were more abundant than those in control groups at 2 weeks posttransplant. Counting the number of $FOXP3^+$ cells in immunostained sections

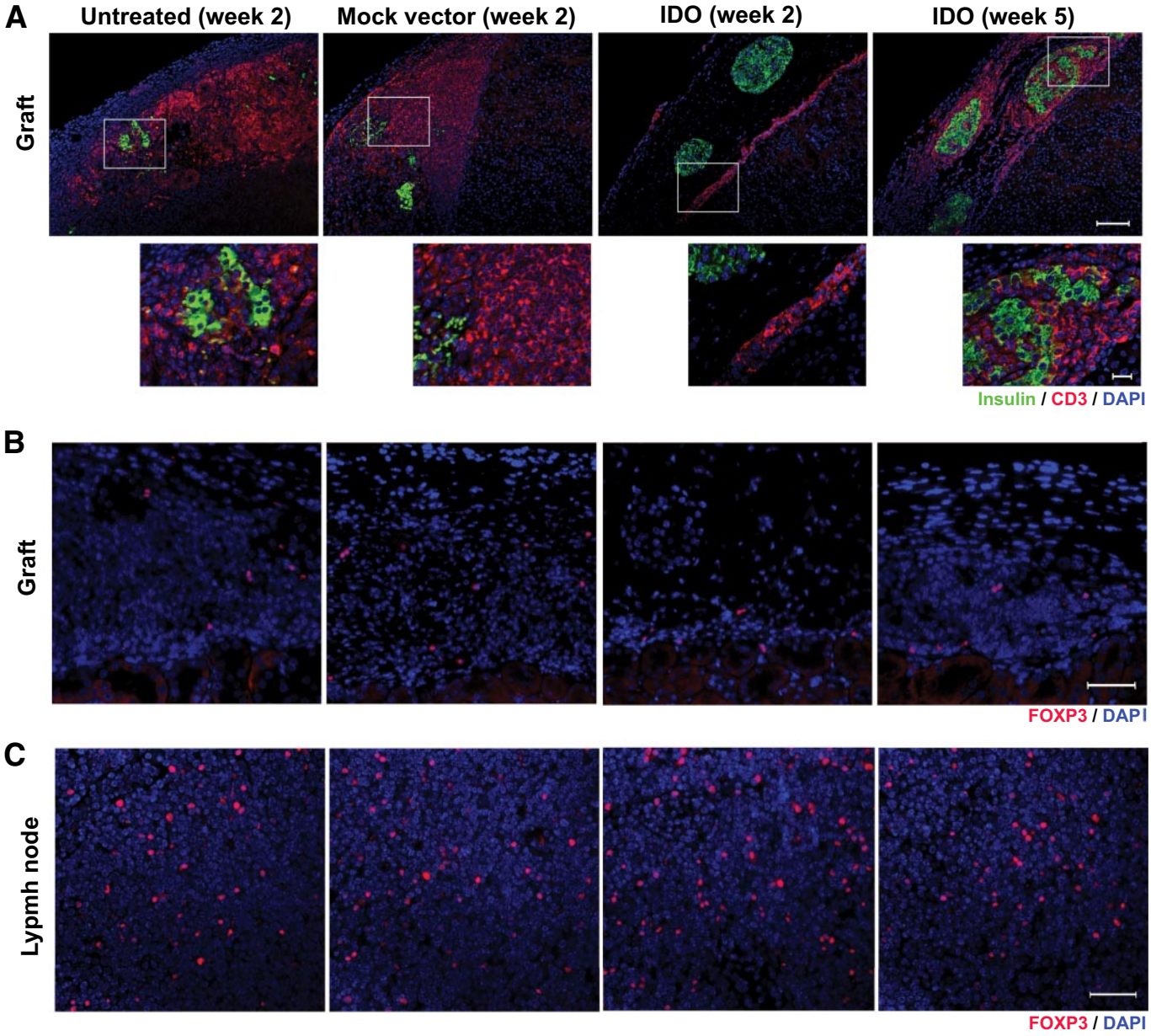

FIG. 3. CD3$^+$ and FOXP3$^+$ cells infiltrating into composite islet grafts and in draining lymph nodes. Graft-recipient mice were killed at indicated time points posttransplantation. Composite islet grafts were then retrieved and subjected to double immunofluorescence staining for CD3 and insulin or FOXP3. *A*: Composite grafts in untreated, mock vector–infected, and IDO-expressing fibroblast graft at 2 weeks posttransplantation and IDO graft after 5 weeks posttransplantation. The *lower panels* show high magnification of the indicated area of the *upper panels*. Note that in the IDO-expressing graft, CD3$^+$ cells accumulated in the border of the graft and kidney tissue but did not infiltrate the graft. Scale bars in the low- and high-magnification panels equal 100 and 20 μm, respectively. *B* and *C*: FOXP3 immunofluorescence staining of composite grafts (*B*) and graft draining lymph nodes (*C*). Untreated, mock vector, and IDO grafts at 2 weeks posttransplantation and IDO grafts after 5 weeks posttransplantation. Scale bar: 50 μm. (A high-quality digital representation of this figure is available in the online issue.)

showed significantly a higher frequency of FOXP3$^+$ cells in the IDO group (9.8 ± 0.9%; $P < 0.001$) compared with untreated (5.6 ± 1.1%) and mock vector (6.2 ± 1.2%) groups (Fig. 6*A*). FOXP3$^+$ cell frequency, however, decreased in the IDO group after 5 weeks (7.0 ± 1.1%; Fig. 7*A*). To investigate the impact of an increased number of FOXP3$^+$ cells and other possible effects of local IDO overexpression on T-cell priming capacity, mixed lymphocyte reactions were performed. The results showed a significant hyporesponsiveness of lymph node cells of IDO-expressing group to stimulation with BALB/c (islet donor) mouse splenocytes but not to a third-party mouse strain (Fig. 6*B* and *C*). This anergy was reverted after 5 weeks posttransplant. These findings suggest that, possibly because of an increased number of regulatory T-cells, antigen-specific incompetence of T-cell priming occurs in draining lymph nodes of IDO-expressing graft–recipient mice.

Duration of IDO transgene expression in composite grafts corresponds to effectiveness of immunosuppression and graft survival length. In view of the limited length of an antirejection effect of IDO in this study, we hypothesized that a decline in the level of IDO transgene expression can be considered a possible cause of cessation of immunosuppression and, eventually, late graft rejection in IDO group. We therefore tested the length of intragraft IDO transgene expression using IDO immunofluorescence staining and quantitative PCR. Composite grafts were harvested at indicated time points and

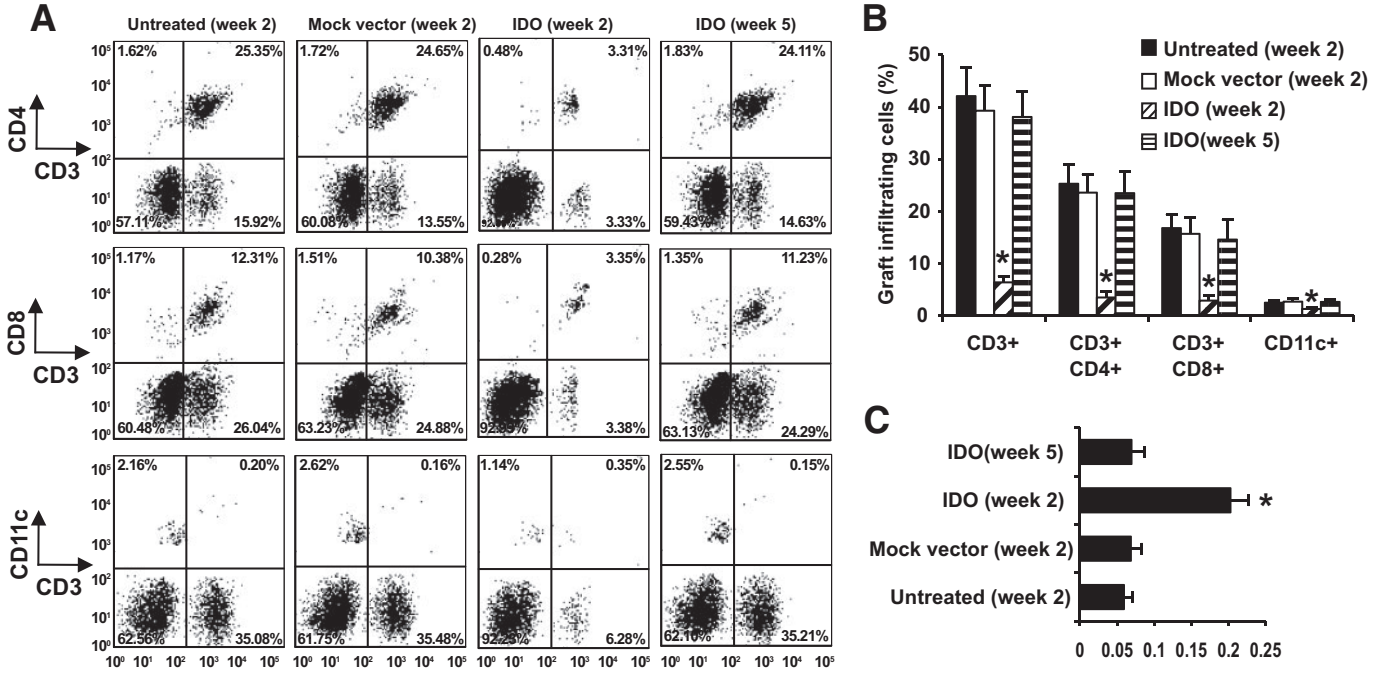

FIG. 4. Characterization of graft-infiltrating cells. Graft-recipient mice were killed at indicated time points posttransplantation. Composite islet grafts were then retrieved and processed as described in RESEARCH DESIGN AND METHODS to prepare single-cell suspensions. Phenotype of cells was then assessed using flow cytometry. *A*: Representative flow cytometry plots comparing $CD4^+$, $CD8^+$, and $CD11c^+$ cells in the grafts. The percent of events in each quadrant of dot plots is indicated. Plots in each row include untreated, mock vector, and IDO grafts at 2 weeks posttransplantation and IDO grafts after 5 weeks posttransplantation. *B*: frequency of $CD3^+$, $CD4^+$, and $CD11c^+$ cells in grafts. *C*: Ratio of $CD11c^+$ to $CD3^+$ cells in grafts. Data are means ± SEM. *Significant difference between IDO (week 2) and other groups ($P < 0.001$; $n = 5$).

subjected to IDO immunofluorescence staining or quantitative PCR (qPCR). As shown in Fig. 7*A*, IDO protein is expressed uniformly and widely in fibroblasts throughout the graft when tested 2 weeks after transplantation. However, after 5 weeks, only a limited number of cells in the graft were still positive for IDO protein (Fig. 7*B*). The anti-IDO antibody used in this experiment was able to detect IDO protein from both human and mouse origins.

qPCR results showed that the IDO transgene was expressed at high levels in composite grafts containing IDO

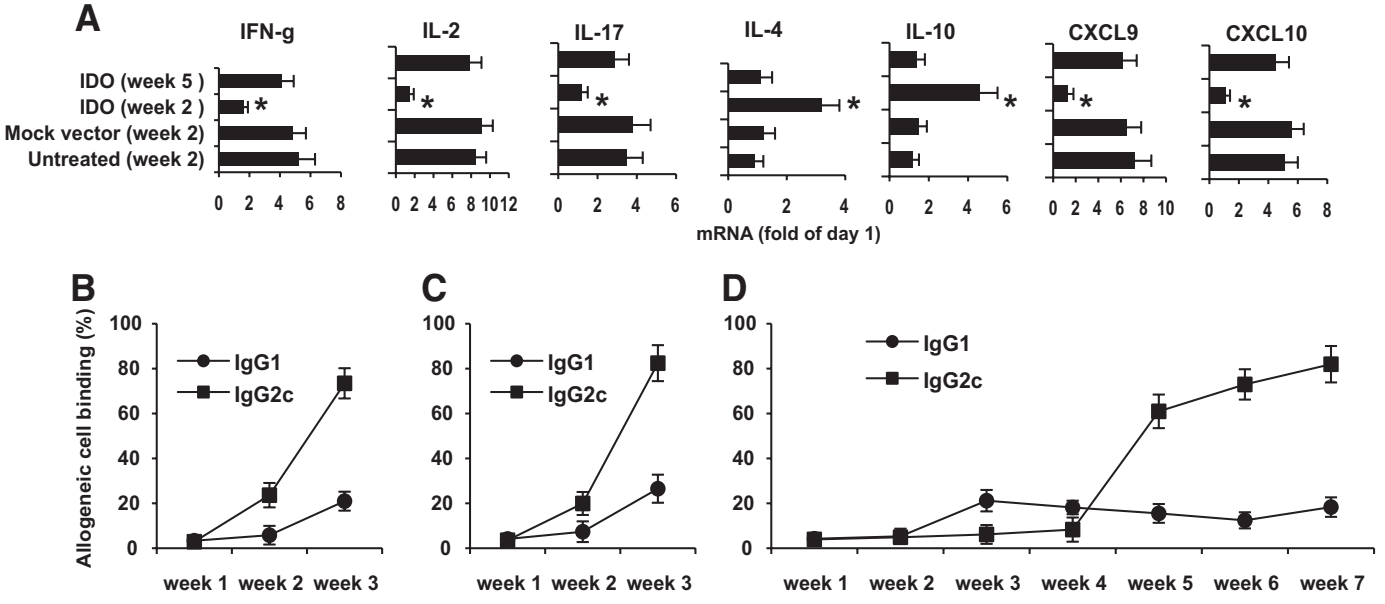

FIG. 5. Cytokine/chemokine expression profile in composite grafts and donor-specific alloantibody production. *A*: Graft-recipient mice were killed at indicated time points posttransplantation. Composite islet grafts were then retrieved and total RNAs were extracted and subjected to qPCR for cytokines γ-interferon, IL-2, IL-17, IL-4, and IL-10 and chemokines CXCL9 and CXCL10. mRNA levels at indicted time points were standardized by mRNA levels on day 1 posttransplant for each experimental group. Data are means ± SEM. *Significant difference between IDO (week 2) and other groups ($P < 0.001$; $n = 5$). *B–D*: Donor-specific alloantibody production in graft-recipient mice. Naïve donor strain BALB/c thymocytes (H-2d) were incubated with serum collected from B6 (H-2b) mice that received graft with untreated (*B*), mock vector–infected (*C*), or IDO-expressing (*D*) fibroblasts on indicated time points after transplantation (week 1–3 for controls and week 1–7 for IDO group). Binding of alloantibody was assessed by flow cytometry analysis after incubation of FITC-conjugated goat anti-mouse IgG1 or anti-mouse IgG2c antibody. The average percentage of donor cells binding to serum antibodies from three individual recipients per group is expressed.

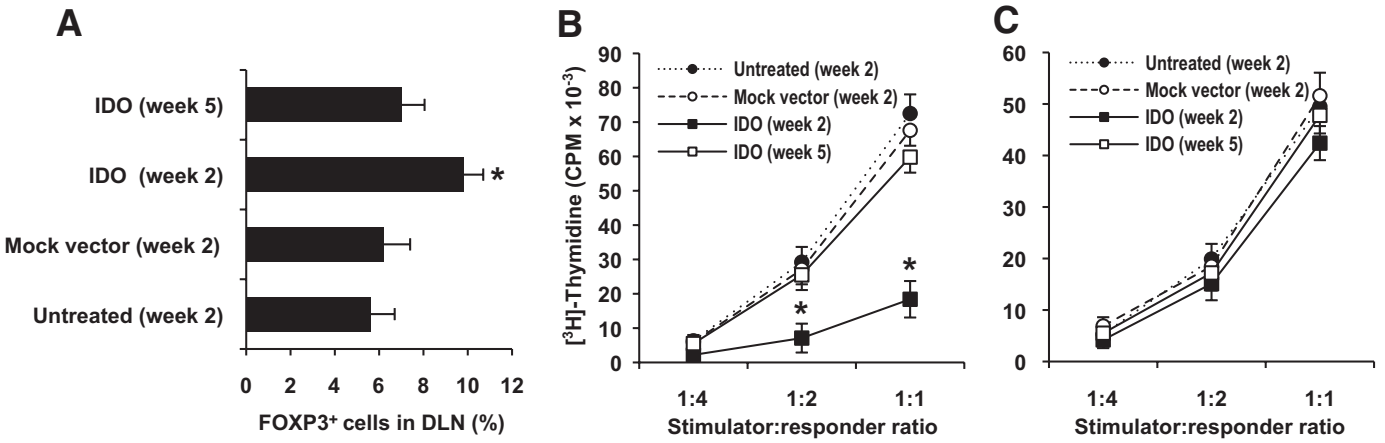

FIG. 6. FOXP3$^+$ cells in draining lymph nodes and mixed lymphocyte reactions. *A*: Frequency of FOXP3$^+$ cells in graft draining lymph nodes were calculated by counting FOXP3 immunostained cells (red cells in Fig. 3*C*) in 10 high-power fields. Data means ± SEM. *Significant difference between IDO (week 2) and other groups ($P < 0.001$; $n = 10$). *B* and *C*: Graft-draining (renal) lymph node cells from graft recipient (B6; H-2b) mice were harvested and cultured with irradiated islet donor (BALB/c; H-2d) mice (*B*) and third-party (C3H; H-2k) (*C*) mice splenocytes at indicated ratios for 96 h. Wells were pulsed with [^{3}H]-thymidine for the last 18 h, and then [^{3}H]-thymidine incorporation to DNA was measured in triplicate. *Significant difference between IDO (week 2) and other groups ($P < 0.001$; $n = 10$).

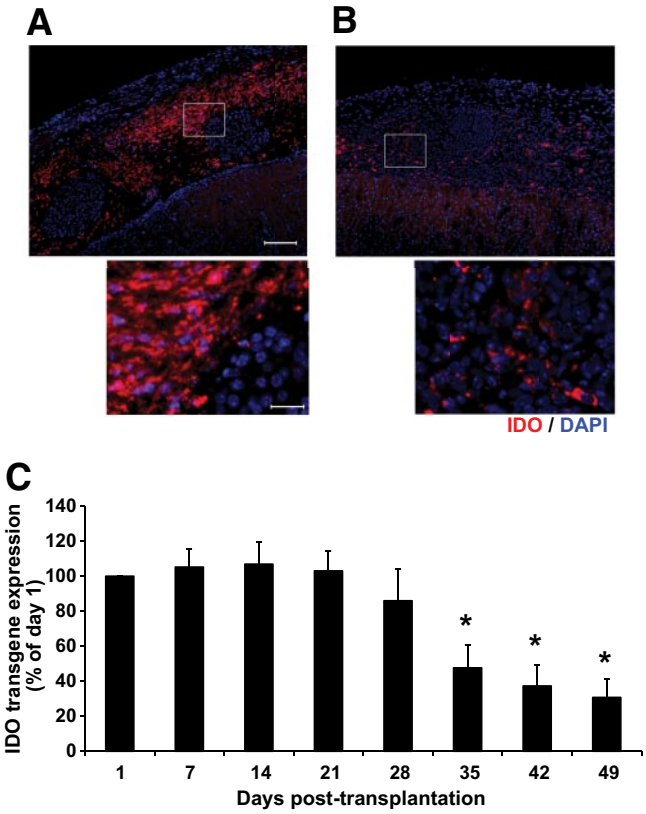

FIG. 7. Stability analysis of IDO transgene expression in composite islet grafts. IDO graft-recipient mice were killed at indicated time points posttransplantation. Composite islet grafts were then retrieved and subjected to immunofluorescence staining or quantitative PCR for IDO. *A* and *B*: Immunofluorescence staining of IDO protein (red) in IDO vector–infected grafts after 2 weeks (*A*) and 5 weeks (*B*) post-transplantation. *Lower panels*: high magnification of the indicated area of the *upper panels*. Scale bars in the low- and high-magnification panels equal 100 and 20 μm, respectively. *C*: IDO transgene mRNA levels measured by quantitative PCR in IDO vector–infected grafts on days 1–49 posttransplantation. The level of IDO mRNA at each time point was normalized as the percentage of IDO mRNA level on day 1 posttransplantation. *Statistically significant difference compared with IDO mRNA level on day 1 posttransplantation ($n = 3$; $P < 0.001$). Error bars indicate SEM. (A high-quality digital representation of this figure is available in the online issue.)

vector–infected fibroblasts for up to 4 weeks posttransplantation; then, the expression level started to decrease. As presented in Fig. 7*C*, significant decline in the intragraft IDO transgene expression were observed from 100% on day one to 47.6 ± 13.4, 37.2 ± 12.3, and 30.6 ± 10.7% on days 35, 42, and 49 posttransplantation, respectively ($P < 0.001$; $n = 3$). This finding was consistent with an in vitro lasting effect of IDO expression in fibroblasts following adenoviral IDO transduction (data not shown). IDO transgene mRNA was not found in the control grafts (data not shown). Because the IDO transgene was of human origin, by using human specific primers we expected that intrinsic IDO expression (i.e., mouse IDO that expressed in grafts as a result of inflammation) did not interfere with IDO transgene qPCR.

These data collectively show a transient pattern for IDO transgene expression in composite grafts following adenoviral gene transfer. The time course of intragraft IDO expression closely corresponds to the duration of graft survival and suppression of cellular and humoral alloimmune responses. We therefore suggest that late graft rejection in this study was probably due to time-dependent loss of transient IDO expression.

DISCUSSION

In the present study, we showed that local IDO expression suppresses cellular and humoral alloimmune responses against islets and significantly prolongs islet allograft survival without systemic anti-rejection treatments in diabetic immune-competent mice. IDO plays a crucial role in suppression of immune responses. Several previous studies implicated an immunomodulatory effect of IDO in different settings including islet transplantation (28,29,37). However, this is the first time that IDO-expressing bystander syngeneic fibroblast–populated collagen scaffold has been used to protect islet allograft. The engineered composite graft developed and transplanted in this study has several unique features. First, we avoided direct transfer of IDO transgene to islets to reduce the risk of cytotoxicity and loss of islet function. There have been reports showing that adenoviral gene transfer to islets interferes with β-cell function and increases apoptosis rate (30–32,38–39). Moreover, gene expression after direct transduction has been observed only in the periphery of islets and not in the islet core (40,41). Therefore,

by using bystander fibroblasts and not islets as the target for IDO gene transfer, we were able to induce high levels of IDO expression as a local immunosuppressive factor while avoiding any deleterious consequence of gene transfer on islet survival and function.

Embedding islets within a three-dimensional extracellular matrix (ECM) is another advantage of this composite graft. ECM is one of the most important constituents of the islet microenvironment. Several studies have demonstrated that entrapment of islets within a collagen matrix results in satisfactory morphology, enhanced viability, and improved insulin secretory capability in islets (42–44). As such, embedding islets within ECM, by itself, can improve islet graft function. Moreover, as shown in supplementary Fig. 1, collagen matrix provides a supportive scaffold and helps IDO-expressing fibroblasts surround and protect islets very efficiently in a three-dimensional structure.

Cotransplantation of fibroblasts is also a beneficial aspect of this composite graft. Fibroblasts are cells of choice to be used as bystander IDO-expressing cells because *1*) they can easily be induced to express IDO, *2*) they show low levels of DNA synthesis and become quiescent when embedded in a collagen matrix (45), and *3*) they are resistant to apoptosis in an IDO-induced low-tryptophan environment (25,27). Fibroblasts can also improve islet cell viability. The essential role of fibroblasts in islet physiological competence has previously been reported, and it was shown that some fibroblast-produced factors can promote islet survival in culture (35,36). In addition, availability of syngeneic or autologous fibroblasts eliminates the risk of immune response against these cells. Collectively, application of this novel composite islet graft can address a number of common obstacles in islet allotransplantation by preventing immunological rejection, reestablishing islet cell-ECM interaction, and improving islet survival and function.

Findings of the present study suggest that there are several mechanisms through which local IDO overexpression mounts its antirejection effects. These include suppression of effector T-cells at the graft site, induction of a Th2 immune response shift, generation of an anti-inflammatory cytokine profile, and an increased number of regulatory T-cells in draining lymph nodes, which results in antigen-specific impairment of T-cell priming. As shown in Figs. 2 and 3, T-cells accumulated at the margins of the IDO-expressing grafts but did not invade or infiltrate islets. This accords with the well-known function of IDO: generation of a low-tryptophan and high-kynurenine microenvironment within which activated T-cells are not able to proliferate and survive. Data presented in the Fig. 1 show that such a microenvironment protects islet grafts rejection but does not negatively affect islet function.

The transient increase in the number of $FOXP3^+$ cells in our model is very similar to the pattern seen in pregnancy-induced tolerance. It has been shown that due to local expression of IDO in maternal-fetal interface, the number of regulatory T-cells increases during early pregnancy, peaking during the second trimester and followed by a decline postpartum (46). In our model, the number of $FOXP3^+$ cells increases as long as local IDO level is high, and upon cessation of IDO overexpression in the grafts the number of $FOXP3^+$ cells decreases. This is similar to Treg downregulation after IDO levels decrease in maternal-fetal interface postpartum.

This study for the first time shows that local IDO expression can inhibit production of donor specific alloantibodies. The mechanism(s) underlying this phenomenon needs further elucidation. It is well documented that humoral response against donor-specific antigens is clearly dependent on help provided by $CD4^+$ T-cells (47). Only $CD4^+$ T-cells recognizing alloantigen through the indirect pathway are able to provide cognate help to allospecific B-cells for the development of alloantibody (48). As such, inhibition of alloantibody production in our study might be due to a T-cell suppressive effect of IDO that significantly reduces the number of donor-specific T-cells and consequently results in insufficient cognate help to B-cells. Moreover, the Th1/Th2 shift seen in humoral immune response in this study may contribute to the IDO-induced deviation of cytokine expression profile given that IL-4 promotes IgG1 isotype switching (49), whereas IFN-γ favors the IgG2a and IgG2c switch (50).

The finite survival of islet grafts in this study may appear discouraging at first glance. However, data presented here clearly show that as long as high levels of intragraft IDO expression was maintained, islet grafts survived and functioned normally and cellular and humoral immune responses against islets were suppressed very efficiently. This finding suggests that long-term protection of islet grafts is feasible if stable IDO expression in bystander fibroblasts is achieved.

In conclusion, the present study proves the feasibility of the development of a viable and functional IDO-expressing composite islet graft and confirms that IDO efficiently and significantly improves islet allograft survival. This promising finding proves that there is a local islet-directed immunosuppressive effect of IDO and sets the stage for development of a nonrejecatable islet allograft using stable IDO induction in bystander fibroblasts. We are currently investigating this approach.

ACKNOWLEDGMENTS

This study was supported by the Canadian Institutes of Health Research. R.B.J. was supported by University of British Columbia Graduate Fellowship (UGF) and Transplantation Scholarship Training awards.

No potential conflicts of interest relevant to this article were reported.

R.B.J. researched data, contributed to discussion, wrote the manuscript, and reviewed and edited the manuscript. F.F. researched data, contributed to discussion, and reviewed and edited the manuscript. A.M.R. researched data and contributed to discussion. R.H. researched data and contributed to discussion. A.M. researched data. B.L. contributed to discussion and reviewed and edited the manuscript. G.L.W. contributed to discussion and reviewed and edited manuscript. A.G. contributed to discussion, wrote the manuscript, and reviewed and edited the manuscript.

The authors are grateful to Dr. Y. Li (University of British Columbia, Vancouver, British Columbia, Canada) for constructing the IDO adenoviral vector. They thank Dr. C. B. Verchere (University of British Columbia) for useful discussion and advice and also Dr. M. K. Levings and A. N. McMurchy (University of British Columbia) for their help with flow cytometry experiments.

REFERENCES

1. Ricordi C, Hering BJ, Shapiro AM, the Clinical Islet Transplantation Consortium. β-cell transplantation for diabetes therapy. Lancet 2008;372:27–28
2. Fiorina P, Secchi A. Pancreatic islet cell transplant for treatment of diabetes. Endocrinol Metab Clin North Am 2007;36:999–1013

3. Froud T, Baidal DA, Ponte G, Ferreira JV, Ricordi C, Alejandro R. Resolution of neurotoxicity and β-cell toxicity in an islet transplant recipient following substitution of tacrolimus with MMF. Cell Transplant 2006;15:613–620
4. Zahr E, Molano RD, Pileggi A, Ichii H, Jose SS, Bocca N, An W, Gonzalez-Quintana J, Fraker C, Ricordi C, Inverardi L: Rapamycin impairs in vivo proliferation of islet β-cells. Transplantation 2007;84:1576–1583
5. Drachenberg CB, Klassen DK, Weir MR, Wiland A, Fink JC, Bartlett ST, Cangro CB, Blahut S, Papadimitriou JC. Islet cell damage associated with tacrolimus and cyclosporine: morphological features in pancreas allograft biopsies and clinical correlation. Transplantation 1999;68:396–402
6. Vantyghem MC, Marcelli-Tourvielle S, Pattou F, Noel C. Effects of non-steroid immunosuppressive drugs on insulin secretion in transplantation. Ann Endocrinol (Paris) 2007;68:21–27
7. Rehman KK, Bertera S, Trucco M, Gambotto A, Robbins PD. Immunomodulation by adenoviral-mediated SCD40-ig gene therapy for mouse allogeneic islet transplantation. Transplantation 2007;84:301–307
8. Bertera S, Crawford ML, Alexander AM, Papworth GD, Watkins SC, Robbins PD, Trucco M. Gene transfer of manganese superoxide dismutase extends islet graft function in a mouse model of autoimmune diabetes. *Diabetes* 2003;52:387–393
9. Olthoff KM, Judge TA, Gelman AE, da Shen X, Hancock WW, Turka LA, Shaked A: Adenovirus-mediated gene transfer into cold-preserved liver allografts: survival pattern and unresponsiveness following transduction with CTLA4Ig. Nat Med 1998;4:194–200
10. Stone TW, Darlington LG. Endogenous kynurenines as targets for drug discovery and development. Nat Rev Drug Discov 2002;1:609–620
11. Mellor AL, Munn DH. IDO expression by dendritic cells: tolerance and tryptophan catabolism. Nat Rev Immunol 2004;4:762–774
12. Mellor A. Indoleamine 2,3 dioxygenase and regulation of T cell immunity. Biochem Biophys Res Commun 2005;338:20–24
13. Bauer TM, Jiga LP, Chuang JJ, Randazzo M, Opelz G, Terness P. Studying the immunosuppressive role of indoleamine 2,3-dioxygenase: tryptophan metabolites suppress rat allogeneic T-cell responses in vitro and in vivo. Transpl Int 2005;18:95–100
14. Munn DH, Zhou M, Attwood JT, Bondarev I, Conway SJ, Marshall B, Brown C, Mellor AL. Prevention of allogeneic fetal rejection by tryptophan catabolism. Science 1998;281:1191–1193
15. Mellor AL, Sivakumar J, Chandler P, Smith K, Molina H, Mao D, Munn DH. Prevention of T cell-driven complement activation and inflammation by tryptophan catabolism during pregnancy. Nat Immunol 2001;2:64–68
16. Munn DH, Mellor AL. Indoleamine 2,3-dioxygenase and tumor-induced tolerance. J Clin Invest 2007;117:1147–1154
17. Munn DH. Indoleamine 2,3-dioxygenase, tumor-induced tolerance and counter-regulation. Curr Opin Immunol 2006;8:220–225
18. Le AV, Broide DH. Indoleamine-2,3-dioxygenase modulation of allergic immune responses. Curr Allergy Asthma Rep 2006;6:27–31
19. Grohmann U, Fallarino F, Bianchi R, Orabona C, Vacca C, Fioretti MC, Puccetti P. A defect in tryptophan catabolism impairs tolerance in nonobese diabetic mice. J Exp Med 2003;198:153–160
20. Ghahary A, Li Y, Tredget EE, Kilani RT, Iwashina T, Karami A, Lin X. Expression of indoleamine 2,3-dioxygenase in dermal fibroblasts functions as a local immunosuppressive factor. J Invest Dermatol 2004;122:953–964
21. Li Y, Tredget EE, Ghaffari A, Lin X, Kilani RT, Ghahary A. Local expression of indoleamine 2,3-dioxygenase protects engraftment of xenogeneic skin substitute. J Invest Dermatol 2006;126:128–136
22. Sarkhosh K, Tredget EE, Uludag H, Kilani RT, Karami A, Li Y, Iwashina T, Ghahary A. Temperature-sensitive polymer-conjugated IFN-γ induces the expression of IDO mRNA and activity by fibroblasts populated in collagen gel (FPCG). J Cell Physiol 2004;201:146–154
23. Sarkhosh K, Tredget EE, Karami A, Uludag H, Iwashina T, Kilani RT, Ghahary A. Immune cell proliferation is suppressed by the interferon-γ-induced indoleamine 2,3-dioxygenase expression of fibroblasts populated in collagen gel (FPCG). J Cell Biochem 2003;90:206–217
24. Sarkhosh K, Tredget EE, Li Y, Kilani RT, Uludag H, Ghahary A. Proliferation of peripheral blood mononuclear cells is suppressed by the indoleamine 2,3-dioxygenase expression of interferon-γ-treated skin cells in a co-culture system. Wound Repair Regen 2003;11:337–345
25. Forouzandeh F, Jalili RB, Germain M, Duronio V, Ghahary A. Skin cells, but not T cells, are resistant to indoleamine 2, 3-dioxygenase (IDO) expressed by allogeneic fibroblasts. Wound Repair Regen 2008;16:379–387
26. Jalili RB, Rayat GR, Rajotte RV, Ghahary A. Suppression of islet allogeneic immune response by indoleamine 2,3 dioxygenase-expressing fibroblasts. J Cell Physiol 2007;213:137–143
27. Jalili RB, Forouzandeh F, Moeenrezakhanlou A, Rayat GR, Rajotte RV, Uludag H, Ghahary A. Mouse pancreatic islets are resistant to indoleamine 2,3 dioxygenase-induced general control nonderepressible-2 kinase stress pathway and maintain normal viability and function. Am J Pathol 2009; 174:196–205
28. Alexander AM, Crawford M, Bertera S, Rudert WA, Takikawa O, Robbins PD, Trucco M. Indoleamine 2,3-dioxygenase expression in transplanted NOD islets prolongs graft survival after adoptive transfer of diabetogenic splenocytes. Diabetes 2002;51:356–365
29. Bertera S, Alexander AM, Crawford ML, Papworth G, Watkins SC, Robbins PD, Trucco M. Gene combination transfer to block autoimmune damage in transplanted islets of langerhans. Exp Diabesity Res 2004;5:201–210
30. Barbu AR, Akusjarvi G, Welsh N. Adenoviral-induced islet cell cytotoxicity is not counteracted by bcl-2 overexpression. Mol Med 2002;8:733–741
31. Potiron N, Chagneau C, Boeffard F, Soulillou JP, Anegon I, Le Mauff B. Adenovirus-mediated CTLA4Ig or CD40Ig gene transfer delays pancreatic islet rejection in a rat-to-mouse xenotransplantation model after systemic but not local expression. Cell Transplant 2005;14:263–275
32. Barbu AR, Akusjarvi G, Welsh N. Adenoviral-mediated transduction of human pancreatic islets: importance of adenoviral genome for cell viability and association with a deficient antiviral response. Endocrinology 2005; 146:2406–2414
33. Pinkse GGM, Bouwman WP, Jiawan-Lalai R, Terpstra OT, Bruijn JA, de Heer E. Integrin signaling via RGD peptides and anti-β1 antibodies confers resistance to apoptosis in islets of langerhans. Diabetes 2006;55:312–317
34. Wang RN, Rosenberg L. Maintenance of β-cell function and survival following islet isolation requires re-establishment of the islet-matrix relationship. J Endocrinol 1999;163:181–190
35. Miki A, Narushima M, Okitsu T, Takeno Y, Soto-Gutierrez A, Rivas-Carrillo JD, Navarro-Alvarez N, Chen Y, Tanaka K, Noguchi H, Matsumoto S, Kohara M, Lakey JR, Kobayashi E, Tanaka N, Kobayashi N. Maintenance of mouse, rat, and pig pancreatic islet functions by coculture with human islet-derived fibroblasts. Cell Transplant 2006;15:325–334
36. Rabinovitch A, Russell T, Mintz DH. Factors from fibroblasts promote pancreatic islet B-cell survival in tissue culture. Diabetes 1979;28:1108–1113
37. Jalili RB, Forouzandeh F, Bahar MA, Ghahary A. The immunoregulatory function of indoleamine 2, 3 dioxygenase and its application in allotransplantation. Iran J Allergy Asthma Immunol 2007;6:167–179
38. Weber M, Deng S, Kucher T, Shaked A, Ketchum RJ, Brayman KL. Adenoviral transfection of isolated pancreatic islets: a study of programmed cell death (apoptosis) and islet function. J Surg Res 1997;69:23–32
39. Zhang N, Schroppel B, Chen D, Fu S, Hudkins KL, Zhang H, Murphy BM, Sung RS, Bromberg JS. Adenovirus transduction induces expression of multiple chemokines and chemokine receptors in murine β-cells and pancreatic islets. Am J Transplant 2003;3:1230–1241
40. Mukai E, Fujimoto S, Sakurai F, Kawabata K, Yamashita M, Inagaki N, Mizuguchi H. Efficient gene transfer into murine pancreatic islets using adenovirus vectors. J Control Release 2007;119:136–141
41. Narushima M, Okitsu T, Miki A, Yong C, Kobayashi K, Yonekawa Y, Tanaka K, Ikeda H, Matsumoto S, Tanaka N, Kobayashi N. Adenovirus mediated gene transduction of primarily isolated mouse islets. ASAIO J 2004;50:586–590
42. Chao SH, Peshwa MV, Sutherland DE, Hu WS. Entrapment of cultured pancreas islets in three-dimensional collagen matrices. Cell Transplant 1992;1:51–60
43. Kaido T, Yebra M, Cirulli V, Rhodes C, Diaferia G, Montgomery AM. Impact of defined matrix interactions on insulin production by cultured human β-cells: effect on insulin content, secretion, and gene transcription. Diabetes 2006;55:2723–2729
44. Nagata N, Gu Y, Hori H, Balamurugan AN, Touma M, Kawakami Y, Wang W, Baba TT, Satake A, Nozawa M, Tabata Y, Inoue K. Evaluation of insulin secretion of isolated rat islets cultured in extracellular matrix. Cell Transplant 2001;10:447–451
45. Rosenfeldt H, Grinnell F. Fibroblast quiescence and the disruption of ERK signaling in mechanically unloaded collagen matrices. J Biol Chem 2000; 275:3088–3092
46. Somerset DA, Zheng Y, Kilby MD, Sansom DM, Drayson MT. Normal human pregnancy is associated with an elevation in the immune suppressive CD25+ CD4+ regulatory T-cell subset. Immunology 2004;112:38–43
47. Taylor AL, Negus SL, Negus M, Bolton EM, Bradley JA, Pettigrew GJ. Pathways of helper CD4 T cell allorecognition in generating alloantibody and CD8 T cell alloimmunity. Transplantation 2007;83:931–937
48. Steele DJ, Laufer TM, Smiley ST, Ando Y, Grusby MJ, Glimcher LH, Auchincloss H Jr. Two levels of help for B cell alloantibody production. J Exp Med 1996;183:699–703
49. Fischer K, Collins H, Taniguchi M, Kaufmann SHE, Schaible UE. IL-4 and T cells are required for the generation of IgG1 isotype antibodies against cardiolipin. J Immunol 2002;168:2689–2694
50. Snapper C, Peschel C, Paul W. IFN-γ stimulates IgG2a secretion by murine B cells stimulated with bacterial lipopolysaccharide. J Immunol 1988;140: 2121–2127